

Probing the Transition State Ensemble of a Protein Folding Reaction by Pressure-Dependent NMR Relaxation Dispersion

Dmitry M. Korzhnev,^{‡,§} Irina Bezsonova,[§] Ferenc Evanics,[§] Nicolas Taulier,^{||}
Zheng Zhou,[⊥] Yawen Bai,[⊥] Tigran V. Chalikian,^{||} R. Scott Prosser,[§] and
Lewis E. Kay^{*,‡,§}

Contribution from the Departments of Medical Genetics and Biochemistry, University of Toronto, Toronto, Ontario, Canada, M5S 1A8, Department of Chemistry, University of Toronto, Toronto, Ontario, Canada, M5S 1A8, Department of Pharmaceutical Sciences, Leslie Dan Faculty of Pharmacy, University of Toronto, Toronto, Ontario, Canada, M5S 2S2, and National Cancer Institute, Laboratory of Biochemistry, Building 37, Bethesda, Maryland 20892

Received January 9, 2006; E-mail: kay@pound.med.utoronto.ca

Abstract: The F61A/A90G mutant of a redesigned form of apocytochrome b_{562} folds by an apparent two-state mechanism. We have used the pressure dependence of ^{15}N NMR relaxation dispersion rate profiles to study the changes in volumetric parameters that accompany the folding reaction of this protein at 45 °C. The experiments were performed under conditions where the folding/unfolding equilibrium could be studied at each pressure without addition of denaturants. The exquisite sensitivity of the methodology to small changes in folding/unfolding rates facilitated the use of relatively low-pressure values (between 1 and 270 bar) so that pressure-induced changes to the unfolded state ensemble could be minimized. A volume change for unfolding of -81 mL mol^{-1} is measured (at 1 bar), a factor of 1.4 larger (in absolute value) than the volume difference between the transition state ensemble (TSE) and the unfolded state. Notably, the changes in the free energy difference between folded and unfolded states and in the activation free energy for folding were not linear with pressure. Thus, the difference in the isothermal compressibility upon unfolding ($-0.11\text{ mL mol}^{-1}\text{ bar}^{-1}$) and, for the first time, the compressibility of the TSE relative to the unfolded state ($0.15\text{ mL mol}^{-1}\text{ bar}^{-1}$) could be calculated. The results argue for a TSE that is collapsed but loosely packed relative to the folded state and significantly hydrated, suggesting that the release of water occurs after the rate-limiting step in protein folding. The notion of a collapsed and hydrated TSE is consistent with expectations based on earlier temperature-dependent folding studies, showing that the barrier to folding at 45 °C is entropic (Choy, W. Y.; Zhou, Z.; Bai, Y.; Kay, L. E. *J. Am. Chem. Soc.* **2005**, *127*, 5066–5072).

An important goal in the study of protein folding is to characterize the energy landscape that directs the folding process.¹ In principle, this is accomplished by probing the structures and dynamics of the conformational states that are formed along the folding pathway^{2,3} and by quantification of the kinetics and thermodynamics of the interconversion between different molecular states that are produced during folding.⁴ Structural studies of the folded state, corresponding to one of the endpoints of the folding reaction, can be performed in a relatively straightforward manner using X-ray crystallography or NMR spectroscopy. In contrast, the ensemble of structures that describes unfolded states is more difficult to characterize

in detail. Nevertheless, some structural and dynamic features of such states can be obtained through spectroscopic and kinetic studies; in particular, solution-based NMR methods have proven very useful in this regard.^{5–7} Insights into the properties of the transition state ensemble (TSE) are difficult to obtain from direct measurements because this ensemble is associated with the highest energy point on the folding pathway. TSEs can be studied, however, via the ϕ -value analysis of Fersht and co-workers that quantifies the sensitivity of the energy of the TSE in response to mutations in the primary protein structure, relative to that of the folded (F) state.⁸ Vendruscolo and co-workers have used such a ϕ -value analysis to generate an ensemble of structures that characterizes the TSE of acylphosphatase and have shown that only a few residues are key for the collapse of this protein.⁹

[‡] Departments of Medical Genetics and Biochemistry, University of Toronto.

[§] Department of Chemistry, University of Toronto.

^{||} Leslie Dan Faculty of Pharmacy, University of Toronto.

[⊥] National Cancer Institute, Laboratory of Biochemistry.

(1) Dinner, A. R.; Sali, A.; Smith, L. J.; Dobson, C. M.; Karplus, M. *Trends Biochem. Sci.* **2000**, *25*, 331–339.

(2) Shortle, D. *Curr. Opin. Struct. Biol.* **1996**, *6*, 24–30.

(3) Feng, H.; Zhou, Z.; Bai, Y. *Proc. Natl. Acad. Sci. U.S.A.* **2005**, *102*, 5026–5031.

(4) Fersht, A. *Structure and Mechanism in Protein Science*; W. H. Freeman and Company: New York, 1999.

(5) Dyson, H. J.; Wright, P. E. *Chem. Rev.* **2004**, *104*, 3607–3622.

(6) Dyson, H. J.; Wright, P. E. *Methods Enzymol.* **2005**, *394*, 299–321.

(7) Bai, Y.; Sosnick, T. R.; Mayne, L.; Englander, S. W. *Science* **1995**, *269*, 192–197.

(8) Matouschek, A.; Kellis, J. T., Jr.; Serrano, L.; Fersht, A. R. *Nature* **1989**, *340*, 122–126.

(9) Vendruscolo, M.; Paci, E.; Dobson, C. M.; Karplus, M. *Nature* **2001**, *409*, 641–645.

The energy landscape is commonly probed through the addition of chemicals such as denaturants⁴ and/or through changes in temperature so that enthalpy, entropy, and heat capacity differences among F, TSE, and U are obtained. The changes in thermodynamic and kinetic parameters that ensue can often be interpreted qualitatively in terms of molecular structure and reflect also on the hydration properties of the various states along the folding pathway. Pressure is another important variable that can be manipulated to obtain insight into protein folding, through quantification of the volumetric changes that accompany the folding transition.^{10–15} However, analysis of changes in free energies and kinetics due to pressure are much less common than the corresponding approaches that make use of either temperature or denaturant-based perturbations. This is unfortunate because changes in folding free energies with pressure provide unique information on the hydration and packing properties of the states that define the folding pathway.

Much of what is known about the volumetric properties associated with protein folding transitions has been derived from density and sound velocity measurements that are performed at atmospheric pressure as a function of some perturbant such as pH or denaturant^{16,17} or from experiments in which high pressure (often to several 1000 bar) is employed as the perturbant.¹² Both types of studies can be problematic. For example, in comparing changes in properties between the folded state measured at one set of conditions with those for the unfolded state obtained under another set of conditions, often significant corrections/extrapolations must be invoked to account for the changes that result from the perturbant.¹⁸ In the case of high-pressure studies, there may be changes in the unfolded state that are introduced by such extreme pressures in the first place.¹⁶

A powerful approach for the study of dynamic systems with motions on the microsecond to millisecond time scale is one that uses relaxation dispersion NMR spectroscopy to probe the interconversion between highly populated (ground) and lowly populated (excited) states. In these experiments, NMR active spin reporters exchange between different chemical environments associated with the exchanging species,¹⁹ leading to line broadening of resultant spectra that can be interpreted in terms of the thermodynamics and kinetics of the exchange process and the structures of the exchanging conformers.²⁰ The excited states need not necessarily be observable (and in most cases are not), although their relative populations must be on the order of 0.5% or higher. We have previously used ¹⁵N spin relaxation dispersion experiments to study the temperature dependence of the millisecond time scale folding rates of a pair of mutational variants of an engineered apocytochrome *b*₅₆₂ molecule and have shown that both fold according to a two-state model.²¹ Here,

we examine the pressure dependence of the folding reaction of one of these mutants using ¹⁵N dispersion spectroscopy. Because the mutant is marginally stable ($\Delta G_{U-F} = G_U - G_F = 2.6$ kcal/mol at 45 °C, 1 bar), the exchange contributions to spin relaxation are considerable so that the folding reaction can be studied directly, without denaturants. The high sensitivity of the dispersion technique to small changes in populations and rates means that low pressures can be employed, obviating the need to consider high-order, free energy pressure terms in the data analysis and minimizing any pressure-induced changes to either of the unfolded or the transition state ensembles; in addition, at the pressures used, little change is expected in the folding mechanism. Analysis of the pressure dependence of folding and unfolding rates over a range from 1 to 270 bar facilitates the extraction of changes in molar volumes among F, TSE, and U. Notably, the pressure dependence of free energy is not linear, which enables one to determine compressibilities of F and TSE relative to U. To our knowledge, this is the first instance of measuring the relative compressibility of the TSE of a folding reaction. The volumetric data are consistent with a collapsed TSE that is loosely packed and hydrated, in good agreement with temperature-dependent studies of the folding reaction.²¹

Materials and Methods

Protein Production. An ¹⁵N-labeled sample corresponding to the F61A/A90G mutant of Rd-apocyt *b*₅₆₂ (a quintuple mutant, M7W/K98I/N99R/H102N/R106G of apocytochrome *b*₅₆₂ that folds into a four helix bundle)²² was prepared according to the methodology described previously.²³ Samples of 1.0 mM protein and 50 mM NaAc-*d*₃, pH 4.8, were used throughout the analysis.

NMR Spectroscopy and Data Analysis. ¹⁵N single quantum Carr–Purcell–Meiboom–Gill (CPMG) dispersion profiles were recorded on ¹⁵N-labeled samples of the F61A/A90G mutant of Rd-apocytochrome *b*₅₆₂ at 45 °C using a Varian Inova 600 MHz spectrometer. The pulse sequence of Tollinger et al. was used.²⁴ Samples were inserted into an NMR sapphire tube (Saint-Gobain Crystals, Milford, New Hampshire) with a 3.0 mm inner diameter and pressurized using helium; 25 pressure points ranging from 1 to 270 bar were obtained. Relaxation dispersion profiles were generated from peak intensities, $I_1(\nu_{\text{CPMG}})$, measured in a series of 17–20 2D ¹H–¹⁵N correlation maps employing 14 values of the CPMG field strength, ν_{CPMG} , ranging from 50 to 1000 Hz, with a constant relaxation time delay, T_{relax} , of 40 ms (two to five duplicate points were recorded for error analysis). Peak intensities were extracted using the MUNIN approach^{25,26} and were converted into effective relaxation rates $R_{2,\text{eff}} = -1/T_{\text{relax}} \ln(I_1(\nu_{\text{CPMG}})/I_0)$, where I_0 is the peak intensity in the reference spectrum obtained with $T_{\text{relax}} = 0$. Uncertainties in $R_{2,\text{eff}}$ values were estimated as $1/T_{\text{relax}} \langle \Delta I_1 \rangle / I_1(\nu_{\text{CPMG}})$, $\Delta I_1 = \sqrt{\sum_{j=1}^N (I_j(\nu_{\text{CPMG}}) - \langle I(\nu_{\text{CPMG}}) \rangle)^2 / (N-1)}$, where the summation is over all N repeats at a given ν_{CPMG} value, $\langle I(\nu_{\text{CPMG}}) \rangle = \sum_{j=1}^N I_j(\nu_{\text{CPMG}}) / N$, and $\langle \Delta I_1 \rangle$ is the average of ΔI_1 over all ν_{CPMG} values for which repeats were obtained. In cases where calculated errors in $R_{2,\text{eff}}$ were less than 2% of the rate, a minimum value of 2% was used. The reproducibility of dispersion profiles was established by repeat experiments for several pressure points. In cases where repeat measurements were performed, data were averaged for the final analysis.

- (10) Seemann, H.; Winter, R.; Royer, C. A. *J. Mol. Biol.* **2001**, *307*, 1091–1102.
- (11) Fuentes, E. J.; Wand, A. J. *Biochemistry* **1998**, *37*, 9877–9883.
- (12) Prehoda, K. E.; Mooberry, E. S.; Markley, J. L. *Biochemistry* **1998**, *37*, 5785–5790.
- (13) Pappenberger, G.; Saudan, C.; Becker, M.; Merbach, A. E.; Kiefhaber, T. *Proc. Natl. Acad. Sci. U.S.A.* **2000**, *97*, 17–22.
- (14) Akasaka, K.; Li, H. *Biochemistry* **2001**, *40*, 8665–8671.
- (15) Akasaka, K. *Biochemistry* **2003**, *42*, 10875–10885.
- (16) Taulier, N.; Chalikian, T. V. *Biochim. Biophys. Acta* **2002**, *1595*, 48–70.
- (17) Chalikian, T. V. *Annu. Rev. Biophys. Biomol. Struct.* **2003**, *32*, 207–235.
- (18) Taulier, N.; Chalikian, T. V. *J. Mol. Biol.* **2001**, *314*, 873–889.
- (19) Palmer, A. G.; Kroenke, C. D.; Loria, J. P. *Methods Enzymol.* **2001**, *339*, 204–238.
- (20) Korzhnev, D. M.; Salvatella, X.; Vendruscolo, M.; Di Nardo, A. A.; Davidson, A. R.; Dobson, C. M.; Kay, L. E. *Nature* **2004**, *430*, 586–590.
- (21) Choy, W. Y.; Zhou, Z.; Bai, Y.; Kay, L. E. *J. Am. Chem. Soc.* **2005**, *127*, 5066–5072.

- (22) Chu, R.; Takei, J.; Knowlton, J. R.; Andrykovitch, M.; Pei, W.; Kajava, A. V.; Steinbach, P. J.; Ji, X.; Bai, Y. *J. Mol. Biol.* **2002**, *323*, 253–262.
- (23) Chu, R.; Pei, W.; Takei, J.; Bai, Y. *Biochemistry* **2002**, *41*, 7998–8003.
- (24) Tollinger, M.; Skrynnikov, N. R.; Mulder, F. A. A.; Forman-Kay, J. D.; Kay, L. E. *J. Am. Chem. Soc.* **2001**, *123*, 11341–11352.
- (25) Orekhov, V. Y.; Ibraghimov, I. V.; Billeter, M. *J. Biomol. NMR* **2001**, *20*, 49–60.
- (26) Korzhnev, D. M.; Ibraghimov, I. V.; Billeter, M.; Orekhov, V. Y. *J. Biomol. NMR* **2001**, *21*, 263–268.

Table 1. Partial Molar Volume (ΔV) and Isothermal Compressibility ($\Delta\kappa_T$) Differences among Folded (F), Transition (\dagger), and Unfolded (U) States of F61A/A90G Rd-apocyt b_{562} (45 °C) along with the Values of Corresponding Equilibrium/Rate Constants at 1 bar Obtained from Fits of Pressure Dependencies of the Unfolding Rate, k_u ($\dagger - F$), the Folding Rate, k_f ($\dagger - U$), and the Equilibrium Constant, $K_{eq} = k_u/k_f$ (U - F)^a

	k_0 (at $P_0 = 1$ bar)	ΔV [mL/mol]	$\Delta\kappa_T$ [mL/(mol bar)]
$\dagger - F$ (k_u)	$25.2 \pm 0.3(0.4) \text{ s}^{-1}$	$-22 \pm 6(9)$	$0.04 \pm 0.04(0.07)$
$\dagger - U$ (k_f)	$1461 \pm 18(20) \text{ s}^{-1}$	$59 \pm 5(6)$	$0.15 \pm 0.04(0.05)$
U - F ($K_{eq} = k_u/k_f$)	$0.0172 \pm 0.0002(0.0003) \text{ s}^{-1}$	$-81 \pm 5(8)$	$-0.11 \pm 0.04(0.05)$

^aUncertainties in the best-fit parameters were obtained by the covariance matrix method or from a bootstrap simulation procedure (brackets)

Extraction of Kinetic Parameters. Relaxation dispersion data for all nonoverlapped cross peaks measured at $n_p = 25$ pressures were fit together to a model of two-site exchange between F and U states using inhouse-written software. Values of the model parameters were obtained by least-squares fits of experimental $R_{2,eff}$ values to theoretical values calculated with analytical expressions described elsewhere.²⁷ Folding and unfolding rate constants k_f and k_u were treated as global parameters, i.e., the same for all residues at a given pressure. Initially, the data for all peaks were processed together assuming that shift differences between folded and unfolded states, $\Delta\varpi$, are independent of pressure. Then, after excluding the residues with $\Delta\varpi < 0.5$ ppm, the data were processed using models that assume either a linear [$\Delta\varpi(P) = \Delta\varpi(P_0) + \Delta\varpi'(P_0)(P - P_0)$] or a quadratic [$\Delta\varpi(P) = \Delta\varpi(P_0) + \Delta\varpi'(P_0)(P - P_0) + \Delta\varpi''(P_0)(P - P_0)^2$] pressure dependence for chemical shift differences, $\Delta\varpi(P)$. For all but one of the peaks, the pressure gradient of $\Delta\varpi < 0.002$ ppm/bar; the outlying peak for which $\Delta\varpi'(P_0) = 0.0025$ ppm/bar was excluded from subsequent analyses. In the final analysis, data for $n_r = 63$ residues at $n_p = 25$ pressures were fit together assuming a quadratic pressure dependence of $\Delta\varpi(P)$, leading to a model with $2n_p + 3n_r + n_p n_r$ adjustable parameters (k_f and k_u values at n_p pressures, $3n_r$ values of $\Delta\varpi(P_0)$, $\Delta\varpi'(P_0)$, and $\Delta\varpi''(P_0)$ with $P_0 = 1$ bar, and $n_p n_r$ intrinsic relaxation rates). The uncertainties in the extracted model parameters were estimated using the covariance matrix method.²⁸ It is noteworthy that the model where $\Delta\varpi(P)$ is described by a second-order polynomial provides statistically significant improvements in fits relative to the models where $\Delta\varpi''(P_0) = 0$ or $\Delta\varpi'(P_0) = \Delta\varpi''(P_0) = 0$ (F -test probabilities that the observed reductions in χ^2 result from chance are $\sim 10^{-12}$).

Variation of Rates with Pressure. The rate constants k_f and k_u and the equilibrium constant $K_{eq} = k_u/k_f$ for the reaction $F \xrightleftharpoons[k_f]{k_u} U$ that were obtained for 25 pressure values, as described above, were subsequently fit to the following set of equations:^{11,12}

$$\begin{aligned} k_f &= A(T) \exp(-\Delta G_{\dagger-U}/(RT)) \\ k_u &= A(T) \exp(-\Delta G_{\dagger-F}/(RT)) \\ K_{eq} &= k_u/k_f = \exp(-\Delta G_{U-F}/(RT)) \end{aligned} \quad (1)$$

where

$$\Delta G_{I-J} = G_I - G_J = \Delta G_{0,I-J} + \Delta V_{I-J}(P - P_0) - 0.5\Delta\kappa_{T,I-J}(P - P_0)^2 \quad (2)$$

where $I, J \in \{F, U, \dagger\}$, F, U, and \dagger denote folded, unfolded, and transition states, respectively, ΔG_0 is the free energy difference at $P_0 = 1$ bar, T is the absolute temperature, and ΔV_{I-J} and $\Delta\kappa_{T,I-J}$ are differences in partial molar volumes and isothermal compressibilities between states I and J, respectively. $A(T) = k_B T \kappa / h$, where k_B , h , and R are Boltzmann's, Planck's, and the universal gas constants and κ is a transmission coefficient. A value of $\kappa = 1.6 \times 10^{-7}$ has been used, as an empirical estimate for protein folding reactions,²⁹ corresponding to

$k_B \kappa / h = 3000 \text{ s}^{-1} \text{ K}^{-1}$; the value of κ has no effect on the parameters of interest (ΔV and $\Delta\kappa_T$). As discussed in the text, terms beyond quadratic in P were not required to fit the pressure dependence of the observed rates. Uncertainties in the extracted parameters (i.e., k_0 , ΔV , and $\Delta\kappa_T$; see Table 1) were estimated using the covariance matrix method²⁸ as well as from a bootstrap simulation.²⁸ In the bootstrap computation, rates and equilibrium constants obtained from the 25 pressure experiments were numbered 1 through 25. Subsequently, 25 random numbers within the range 1–25 were generated, and the rate/equilibrium constants with the corresponding numbers were selected and analyzed as described above. The process was repeated 100 times, with values for ΔV and $\Delta\kappa_T$ reported as averages and errors reported as standard deviations. In general, the bootstrap method results in uncertainties somewhat higher than those calculated from the covariance matrix (Table 1).

The approach described above for estimating volumetric parameters is based on a two-step procedure where the rate and equilibrium constants k_f , k_u , and K_{eq} (and their uncertainties) are first extracted from relaxation dispersion data and then subsequently fit to obtain ΔV and $\Delta\kappa_T$ values. It is also possible to fit the dispersion data directly to rate expressions that include the effects of pressure, eqs 1 and 2, to extract $\Delta V_{\dagger-F}$, $\Delta V_{\dagger-U}$, $\Delta\kappa_{T,\dagger-F}$, $\Delta\kappa_{T,\dagger-U}$, $k_f(P_0)$, and $k_u(P_0)$, and in this case, values that are very similar to those obtained using the procedure outlined above were obtained.

To establish that the relaxation dispersion profiles measured over the complete pressure range (1–270 bar) are consistent with a two-site exchange process, we have performed the following analysis. Dispersion data recorded from 1 to 270 bar were fit simultaneously *on a per-residue basis* (i.e., each residue is fit independently) to a two-site model of exchange, without any assumptions as to the pressure dependence of the rates, where the chemical shift difference between sites, $\Delta\varpi$, is assumed to vary quadratically with pressure. The fitting process is repeated for each residue 50 times using a jackknife procedure^{21,28} where approximately 30% of the dispersion data is eliminated for each pressure. In this way, a distribution of (k_f, k_u) pairs is obtained from all fits and for all residues considered (18 for which $\Delta\varpi > 2.5$ ppm) at each pressure. Note that this fitting process makes no assumptions about the global nature of the exchange process (i.e., whether it is two-state or not). To estimate the effects of error on the distributions of (k_f, k_u) values that were generated, dispersion data sets were *simulated* assuming that *all residues are involved in a two-state exchange process*. In these computations, the rate constants and chemical shift differences employed were those obtained from the global fit of the experimental data. Dispersion profiles for each residue at a given pressure were constructed with the same (k_f, k_u) values and Gaussian noise on the basis of the estimated experimental errors added to the data. Subsequently, rates were extracted from the synthetic data using exactly the same jackknife procedure as that used for the experimental data, and the distribution of (k_f, k_u) values that derives from a two-state process (with noise) was compared to those rates obtained from experiment, where no assumption about the global exchange process was made in the analysis. A similar distribution of rates obtained from a per-residue analysis of the experimental data and

(27) Korzhnev, D. M.; Kloiber, K.; Kay, L. E. *J. Am. Chem. Soc.* **2004**, *126*, 7320–7329.

(28) Press, W. H.; Flannery, B. P.; Teukolsky, S. A.; Vetterling, W. T. *Numerical Recipes in C*; Cambridge University Press: Cambridge, 1988.

(29) Hagen, S. J.; Hofrichter, J.; Szabo, A.; Eaton, W. A. *Proc. Natl. Acad. Sci. U.S.A.* **1996**, *93*, 11615–11617.

from evaluation of data produced using a two-state model (with errors) indicates strongly that the experimental profiles are consistent with a simple exchange model of the form $F \rightleftharpoons U$ (see Results and Discussion).

Volumetric Measurements. All measurements were performed at 45 °C, varying the pH from 5 to 1.5 (absolute error of ± 0.01 pH unit). The protein concentrations used varied between 0.7 and 1.2 mg/mL.

Volume measurements were obtained using an Anton Paar model DMA 5000 vibrating tube densimeter (Gratz, Austria), as described previously.¹⁸ The partial molar volume of F61A/A90G, V ($\text{cm}^3 \text{mol}^{-1}$), was calculated according to

$$V = \frac{M}{\rho_0} - \frac{(\rho - \rho_0)}{(\rho_0 C)} \quad (3)$$

where ρ and ρ_0 are the densities of the solution and solvent, respectively, M is the molecular weight of the solute, and C is the molar concentration of the solution.³⁰

Sound velocity measurements were carried out at 7.2 MHz using an ultrasonic resonator cell with lithium niobate piezotransducers, as described previously.¹⁸ The partial molar adiabatic compressibility ($\text{mL mol}^{-1} \text{bar}^{-1}$) of the measured solution is given by

$$\kappa_S = \beta_S \left(2V - 2[U] - \frac{M}{\rho} \right) \quad (4)$$

where $[U] = (U - U_0)/(U_0 C)$, with U and U_0 being the measured sound velocities in the solution and solvent, respectively, and $\beta_S = 4.28 \times 10^{-5} \text{bar}^{-1}$.

Changes in partial molar volumes and adiabatic compressibilities resulting from pH-induced protein unfolding derive from two terms: one that reflects the change in volume/compressibility due to the pH-induced change in protein conformation and a second term due to pH-dependent changes in the ionization states of titrating groups on the protein. Contributions from (de)ionization have been taken into account so that $\Delta V(\text{pH})$ and $\Delta \kappa_S(\text{pH})$ profiles (see below) derive from the unfolding event exclusively. The analysis follows the procedure described in detail by Taulier and Chalikian.¹⁸

Results and Discussion

Folding Reaction of F61A/A90G Rd-apocyt b_{562} . In a previous study, ¹⁵N relaxation dispersion experiments have been performed on the F61A/A90G mutant of a redesigned apocytocrome b_{562} protein (see the Materials and Methods section), over a range of temperatures extending from 37.5 to 47.5 °C and at atmospheric pressure.²¹ The majority of residues in the protein ($\sim 60\%$ of the well-resolved correlations) had measurable dispersion profiles. An analysis of the data confirmed that the exchange process responsible for the observed dispersions was due to the folding/unfolding reaction of the protein. For example, large differences in chemical shifts between exchanging states were noted (ranging from 1 to 7 ppm), consistent with a folding reaction, and the change in free energy between states from the dispersion data was in agreement with the free energy of folding determined from thermal melt experiments. In addition, the folding process was shown to be two-state over the range of temperatures examined. The temperature dependence of the exchange parameters was used to obtain a subset of the thermodynamic parameters that characterize the folding reaction. Here, we study the pressure dependence of the folding reaction of F61A/A90G Rd-apocyt b_{562} which allows us to extract volumetric properties of the system and to significantly extend our understanding of the TSE.

Prior to any analysis of the pressure data, it is necessary to establish that the two-state folding behavior observed at a pressure of 1 bar is maintained throughout the pressure series employed here. In principle, if a single dominant exchange process is responsible for the observed dispersion profiles, such as would be the case for the folding reaction $F \rightleftharpoons U$, then fits of dispersion profiles on a per-residue basis to a two-site model of exchange will produce (k_f, k_u) values for each site that are the same (in the absence of error). In contrast, if the exchange process is more complex, then a significant variation in rates will be observed between sites that is well outside what is expected on the basis of the random errors in the data. In the case of the folding reaction of G48 mutants of the Fyn SH3 domain, for example, site specific differences in the rates on the order of a factor of 10 were noted, well outside experimental errors, consistent with a folding process that is more complex than two-site,²⁰ whereas for the F61A/A90G Rd-apocyt b_{562} mutant studied here, the variation in rates observed at a pressure of 1 bar could all be explained by experimental error.²¹

The distribution in (k_f, k_u) values observed for F61A/A90G Rd-apocyt b_{562} as a function of pressure is shown in Figure 1a–d. Here, dispersion data recorded over the complete pressure range (1–270 bar) are fit simultaneously *on a per-residue basis* (i.e., each residue is fit independently) to a two-site model of exchange as described in the Materials and Methods section. To estimate the effects of error on the distribution of (k_f, k_u) values, dispersion data sets were simulated assuming that *all residues are involved in a two-state exchange process*, using parameters at each pressure from the global fit of the experimental data and errors estimated from experiment. Rates were extracted using exactly the same procedure as that for the experimental data and the distribution of (k_f, k_u) values plotted in Figure 1a'–d'. A comparison of the distributions of rates obtained from experimental and simulated data (where a global two-site model of exchange has been explicitly assumed) establishes that the dispersion profiles measured over the complete pressure range examined in the present study can be explained by a two-site process with the range of rates accounted for by experimental errors.

Relaxation Dispersion Spectroscopy as a Function of Pressure. As described in the Materials and Methods section and elsewhere,^{11,12} by measuring the pressure dependencies of the folding and unfolding rates, k_f , k_u , and $K_{\text{eq}} = k_u/k_f$ for the reaction $F \rightleftharpoons U$, it becomes possible, in principle, to extract changes in partial molar volumes, ΔV_{I-J} , and compressibilities, $\Delta \kappa_{T,I-J}$, where $I, J \in \{F, U, \ddagger\}$ and \ddagger denotes the transition state ensemble. As we discuss below, such measures are exquisitely sensitive to hydration and packing while also providing insight into the nature of the folding TSE.

Figure 2a shows ¹⁵N relaxation dispersion curves of several residues from F61A/A90G Rd-apocyt b_{562} in addition to the corresponding region from the ¹H–¹⁵N correlation map ($T = 45$ °C, $P = 1$ bar, 600 MHz spectrometer frequency; inset to Figure 2). Note that only amide correlations from the folded state of the protein are observed in spectra because the unfolded ensemble is populated at less than 2% and is very significantly broadened from exchange. The solid lines in the figure correspond to fits of the experimental data (open circles) that were generated by a simultaneous analysis of all dispersion profiles

(30) Kupke, D. W. In *Physical Principles and Techniques of Protein Chemistry*; Loch, S. J., Ed.; Academic Press: New York, 1973; pp 1–75.

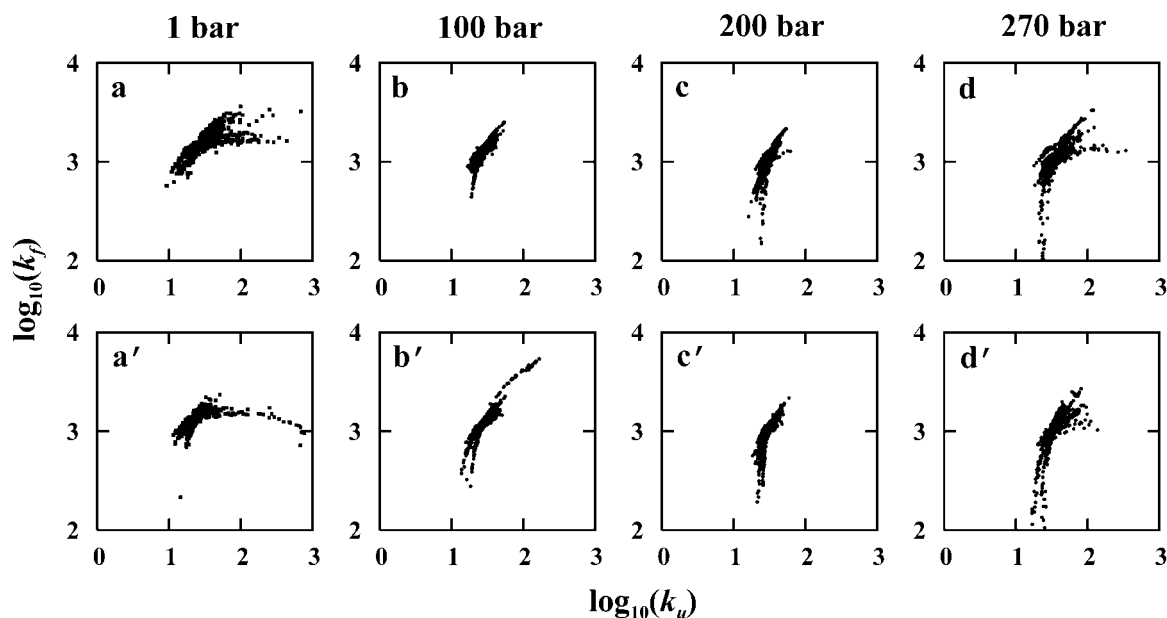


Figure 1. Distributions of (k_f, k_u) values for F61A/A90G Rd-apocyt b_{562} , at 45 °C, as a function of pressure. For each residue used in the analysis, a jackknife procedure was employed to estimate distributions of rates from the experimental data (a–d) and compared with the distributions obtained from simulations where a global two-site exchange model was explicitly used, along with parameters for exchange rates and chemical shift differences from global two-state fits of the experimental data, as described in the text (a'–d'). Rates for all residues considered in the analysis are included in the figure.

to obtain a global set of exchange parameters, as described in the Materials and Methods section. Excellent fits are obtained, with $\chi^2_{\text{reduced}} = 0.8$, establishing further that the two-state model of exchange is appropriate for the analysis of the data. Figure 2b shows the pressure dependence of the dispersion curves from correlation 1 in Figure 2a, for pressures ranging from 1 to 270 bar (additional profiles are shown in the Supporting Information). It is clear that the profiles are very sensitive to pressure, with $R_{\text{ex}} = R_{2,\text{eff}}(50 \text{ Hz}) - R_{2,\text{eff}}(1000 \text{ Hz})$ increasing from 12.0 to 21.5 s^{-1} for peak 1 as the pressure is incremented from 1 to 270 bar.

The pressure dependence of $R_{2,\text{eff}}(\nu_{\text{CPMG}})$, illustrated in Figure 2b, follows directly from the pressure dependencies of k_f and k_u , shown in Figure 3a. Here, k_f (or equivalently, $\Delta G_{\ddagger-U}$) and k_u (ΔG_{U-F}) are obtained at each pressure value from fits of the dispersion curves for all residues in the protein with measurable dispersions (see the Materials and Methods section). Subsequently, $k_f(P)$ and $k_u(P)$ and their ratio, $K_{\text{eq}} = k_u/k_f$, are fit to eqs 1 and 2 (solid lines). Noticeable curvature in the $\Delta G_{\ddagger-U}$ and ΔG_{U-F} vs pressure profiles is observed, indicating that $\Delta\kappa_{T,\ddagger-U} \neq 0$ and $\Delta\kappa_{T,U-F} \neq 0$. Indeed, F -test analyses establish that the model that takes into account compressibility differences between states, $\Delta\kappa_T$, is justified (relative to the case where $\Delta\kappa_T = 0$) in the descriptions of the pressure dependencies of $K_{\text{eq}} = k_u/k_f$ and k_f but not of k_u (probabilities that the observed reductions in χ^2 are due to chance are 7×10^{-3} , 4×10^{-4} , and 0.3, respectively). Finally, fitting the experimental data to expressions for $\Delta G(P)$ that include $\partial\Delta\kappa_T/\partial P$ (i.e., terms higher in order than quadratic in P) is not justified for $\Delta G_{\ddagger-U}$, $\Delta G_{\ddagger-F}$, or ΔG_{U-F} .

Figure 3b illustrates the differences in partial molar volume values among states $\{F, U, \ddagger\}$ estimated on the basis of the fits of k_f and k_u described above, with the distributions obtained from bootstrap simulations, described in the Materials and Methods section. It is clear that $V_U < V_{\ddagger} < V_F$. Figure 3c shows the corresponding changes in isothermal compressibilities

between states. Here, $\kappa_{T,F}$, $\kappa_{T,\ddagger} > \kappa_{T,U}$; the data are not sufficiently accurate to establish the sign of $\Delta\kappa_{T,\ddagger-F}$ because κ_T values of the F and \ddagger states (± 1 standard deviation) overlap extensively (see also Table 1).

Table 1 lists the extracted values of ΔV_{I-J} and $\Delta\kappa_{T,I-J}$, $I, J \in \{F, U, \ddagger\}$, generated as described in the Materials and Methods section. The ΔV_{U-F} value of $-81 \pm 8 \text{ mL/mol}$ is in reasonably good agreement with the value of $-102 \pm 3 \text{ mL/mol}$ that Fuentes and Wand estimated on the basis of a pressure-dependent study of wild-type (WT) apocytochrome b_{562} over a pressure range extending from 1 to 1200 bar, at 27 °C.¹¹ The decrease in the absolute value of ΔV observed here may well reflect the seven mutations in F61A/A90G Rd-apocyt b_{562} relative to the WT protein and the fact that the temperature used in the present study is approximately 20 °C higher. Changes in ΔV_{U-F} values with increasing temperature have been measured for several proteins and have been found to be positive (i.e., ΔV_{U-F} becomes less negative with temperature), mainly because at higher temperature the volumetric differences between the water of protein hydration and bulk water become less pronounced.¹⁷

The compressibility of the U state is less than that obtained for either \ddagger or F (Table 1). The value of $\Delta\kappa_{T,U-F} = -0.11 \pm 0.05 \text{ mL mol}^{-1} \text{ bar}^{-1} = -9.5 \pm 4.3 \times 10^{-6} \text{ mL g}^{-1} \text{ bar}^{-1}$ for F61A/A90G Rd-apocyt b_{562} , at 45 °C, is in qualitative agreement with changes in adiabatic compressibilities measured for the native to fully unfolded transitions of ribonuclease A ($-18 \times 10^{-6} \text{ mL g}^{-1} \text{ bar}^{-1}$, pH 2, 15 °C, GuHCl-induced denatured state)³¹ and lysozyme ($-11 \times 10^{-6} \text{ mL g}^{-1} \text{ bar}^{-1}$, pH 4.0, 25 °C, GuHCl-induced denaturation).³² It is worth noting that what is measured in the present study is an isothermal, not an adiabatic, compressibility difference. However, for a given protein, the calculated differences between the two are not expected to be more than a few percent of either value.¹⁶ It is

(31) Tamura, Y.; Gekko, K. *Biochemistry* **1995**, *34*, 1878–1884.

(32) Kamiyama, T.; Gekko, K. *Chem. Lett.* **1997**, 1063–1064.

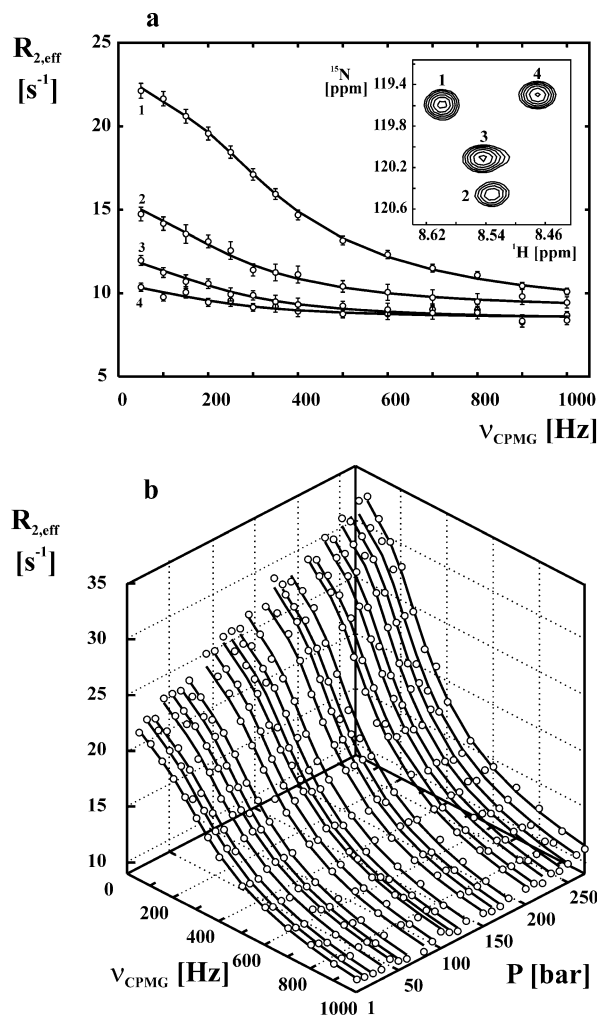


Figure 2. (a) Typical fits of ^{15}N relaxation dispersion profiles recorded on a sample of F61A/A90G Rd-apocyt b_{562} at 1 bar, 600 MHz spectrometer field, and 45 °C for four peaks in a selected region of the ^1H - ^{15}N correlation spectrum (shown in the inset). The HSQC spectrum of the mutant has not been assigned. (b) Pressure dependence of relaxation dispersion profiles for peak 1 of plot a.

thus surprising that positive values of $\Delta\kappa_{\text{T,U-F}}$ (isothermal compressibilities) associated with pressure-induced denaturation have been measured for a number of proteins previously, and negative adiabatic compressibility differences ($\Delta\kappa_{\text{S,U-F}}$) are obtained.¹⁶ As we describe below, it is difficult to unequivocally rationalize the positive values of $\Delta\kappa_{\text{T,U-F}}$, both in terms of simple physical models and on the basis of theory that predicts $\Delta\kappa_{\text{S,U-F}} \sim \Delta\kappa_{\text{T,U-F}}$. The negative value of $\Delta\kappa_{\text{T,U-F}}$ obtained for F61A/A90G Rd-apocyt b_{562} by the relaxation dispersion methodology that is consistent with expectations is thus an important result. Finally, although our data only permit us to state that the compressibilities of \ddagger and F are similar, it is clear that the compressibility of \ddagger is greater than that for U ($\Delta\kappa_{\text{T,}\ddagger\text{-U}} = 0.15 \text{ mL mol}^{-1} \text{ bar}^{-1}$). To our knowledge, this is the first time that the relative compressibility of a transition state ensemble in a folding reaction has been obtained.

Comparison with Values from Densimetric and Sound Velocity Measurements. Figure 4 shows changes in partial molar volumes (a) and compressibilities (b) for F61A/A90G Rd-apocyt b_{562} as a function of pH, after first correcting for contributions from changes in ionization states of titrating groups.¹⁸

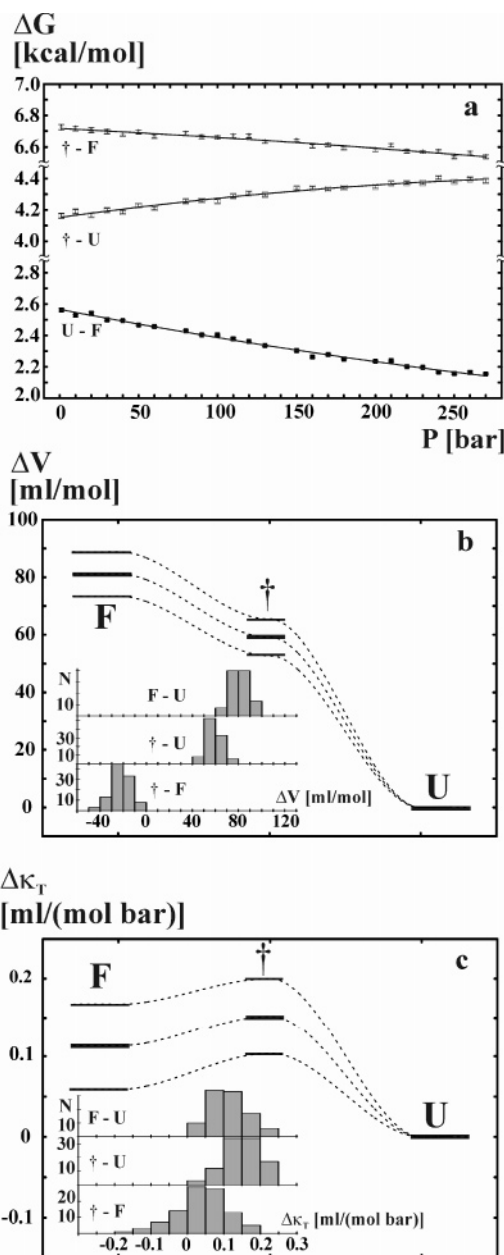


Figure 3. Volumetric properties describing the folding reaction of F61A/A90G Rd-apocyt b_{562} , at 45 °C, by relaxation dispersion NMR spectroscopy. (a) Pressure dependence of the free energy difference between \ddagger and F, $\Delta G_{\ddagger\text{-F}}$ (triangles), \ddagger and U, $\Delta G_{\ddagger\text{-U}}$ (open boxes) and U and F, $\Delta G_{\text{U-F}}$ (filled boxes) from k_u , k_f , and $K_{\text{eq}} = k_u/k_f$ values, respectively. Fits of $\Delta G_{\ddagger\text{-F}}$, $\Delta G_{\ddagger\text{-U}}$, and $\Delta G_{\text{U-F}}$ to eqs 1 and 2 are shown by solid lines. (b) Partial molar volume changes and (c) isothermal compressibility changes of the system as a function of the folding/unfolding coordinate based on the best fits of $\Delta G_{\ddagger\text{-F}}$, $\Delta G_{\ddagger\text{-U}}$, and $\Delta G_{\text{U-F}}$ values (central line denotes the best-fit values, outer lines enclose the region within one standard deviation), referenced to the volume and compressibility of the U state, respectively. Insets show distributions of the volume and compressibility differences between F and U, \ddagger and U, and \ddagger and F from 100 starts of a bootstrap simulation (see the Materials and Methods section).

A $\Delta V_{\text{U-F}}$ value of $-228 \pm 29 \text{ mL/mol}$ is obtained from density measurements, over a factor of 2 larger than that obtained from the pressure/relaxation dispersion study reported here or from the pressure/hydrogen exchange experiments on WT apocyt b_{562} of Fuentes and Wand.¹¹ *Why are such large differences observed?* Insight can be obtained by considering the factors that influence $\Delta V_{\text{U-F}}$ in the first place. We have

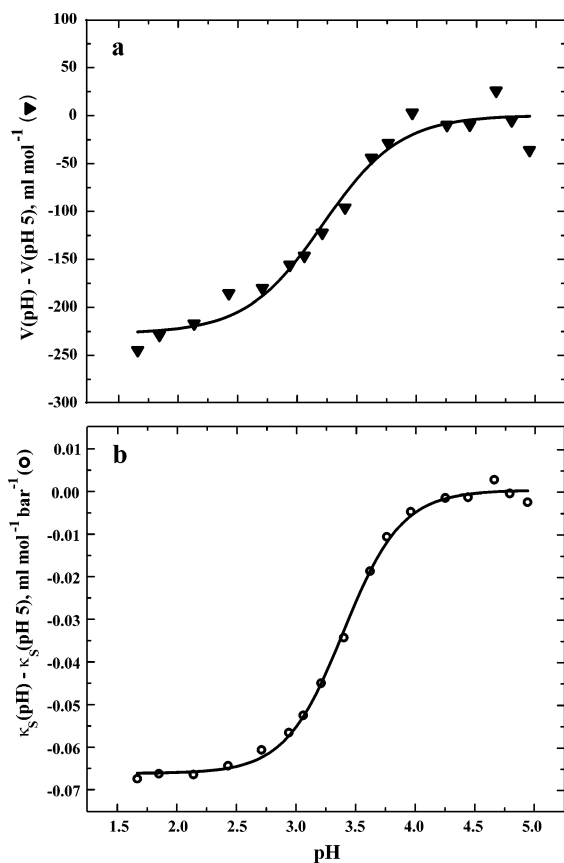


Figure 4. Volumetric properties describing the folding reaction of F61A/A90G Rd-apocyt b_{562} , at 45 °C, by density and sound velocity measurements, as described in the text. (a) Changes in partial molar volume, V , and (b) partial molar adiabatic compressibility, κ_s , as a function of pH.

recently presented a model in which the partial molar volume of a protein, V , is given by the sum of three dominant terms^{17,33}

$$V = V_M + V_I + V_T \quad (5)$$

where V_M is the intrinsic volume of the protein, V_I is the interaction volume that describes the contraction of water in the vicinity of charged and polar groups of the protein (relative to the bulk), and V_T is the thermal volume that exists around the protein due to the mutual thermal vibrations of protein and water. Values of ΔV_M and ΔV_I are negative for the unfolding reaction, whereas ΔV_T is positive; these contributions largely cancel so that for a given protein ΔV_{U-F} does not exceed 1–2% of its partial molar volume.³³ The fact that ΔV_{U-F} derives from large terms that nearly cancel implies that subtle changes in the unfolded state ensemble as a function of pH, for example, could lead to significant changes in ΔV_{U-F} . It is thus very likely that differences in ΔV_{U-F} values among the different types of measurements reported here reflect differences in structural and hydration properties of the U state ensemble between pH 1.5 (U state in the case of density measurements where the perturbant is pH) and 4.8 (U state conditions for the dispersion experiments where the perturbant is pressure). In this regard, experiments that measure volumetric properties with all states in equilibrium and with minimal perturbation (such as low values of pressure) have distinct advantages.

(33) Chalikian, T. V.; Filfil, R. *Biophys. Chem.* **2003**, *104*, 489–499.

A value of $-0.066 \pm 0.002 \text{ mL mol}^{-1} \text{ bar}^{-1}$ is obtained for the adiabatic compressibility, $\Delta\kappa_{S,U-F}$, of F61A/A90G Rd-apocyt b_{562} from sound velocity measurements; by comparison, $\Delta\kappa_{T,U-F} = -0.11 \pm 0.04 \text{ mL mol}^{-1} \text{ bar}^{-1}$ is measured from the dispersion technique. As described above, in many previous studies involving the use of high pressures to perturb the folding equilibrium, positive values of $\Delta\kappa_{T,U-F}$ have been reported.¹⁶ In contrast, our measured values of $\Delta\kappa_{S,U-F}$ and $\Delta\kappa_{T,U-F}$ suggest strongly that, at least in the case of F61A/A90G Rd-apocyt b_{562} , unfolding is accompanied by a decrease in compressibility. In general, the net change in compressibility associated with an unfolding transition depends on differences in both intrinsic and hydration compressibilities between F and U states. We have presented a model that allows one to calculate such changes.¹⁶ In particular, the intrinsic compressibility of a fully unfolded (random coil-like) state is reduced relative to the F state because for a fully unfolded protein κ_T is essentially given by the compressibility of the covalent structure (i.e., bonds), whereas a folded protein is characterized by packing defects that can be “compressed out” with pressure. In addition, the hydration contribution to the compressibility of a fully or partially unfolded state has been estimated to be significantly more negative than that of the F state. This follows from the fact that the extent of hydration is assumed to be proportional to surface area that scales as M (M = molecular weight) and $M^{0.76}$ for the fully unfolded and folded conformations, respectively, and because the hydration sphere is less compressible than bulk water.¹⁶ Thus, the negative values for $\Delta\kappa_{U-F}$ measured here are in keeping with expectations based on simple physical models. In other studies on systems where $\Delta\kappa_{U-F} > 0$, it may well be that what is assumed to be the unfolded ensemble has features that are characteristic of molten globules, possibly due to the use of high pressures.¹⁶ Previous studies have shown that changes in compressibilities associated with native to molten globule transitions are positive, reflecting the increase in the intrinsic compressibilities of such structures mainly due to their loose packing.^{31,34}

Interpretation of ΔV and $\Delta\kappa$ in Terms of Structural Differences of F,U, and † in F61A/A90G Rd-apocyt b_{562} . Figure 3a shows that the stability of the folded state decreases in relation to the unfolded ensemble with increasing pressure over the complete pressure range examined. This implies that at the pressures examined here, $\Delta V_{U-F} < 0$. A decrease in the volume of the U state relative to F is most often rationalized in terms of effects related to packing defects in the F state that are eliminated upon unfolding, exposure to solvent involving previously buried moieties, and an overall increase in hydration of the U state (relative to F).³⁵ The volumetric parameters obtained from the measurements on F61A/A90G Rd-apocyt b_{562} allow several qualitative statements to be made regarding the structure of the TSE. A ϕ -value analysis of the structure of the TSE of this protein based on the protein engineering method provides a picture of an ensemble of loosely packed structures relative to the F state.³⁶ In principle, this gives rise to a positive contribution to $\Delta V_{\ddagger-F}$ which must be offset by a negative contribution from hydration, leading to the observed negative

(34) Chalikian, T. V.; Gindikin, V. S.; Breslauer, K. J. *J. Mol. Biol.* **1995**, *250*, 291–306.

(35) Weber, G.; Drickamer, H. G. *Q. Rev. Biophys.* **1983**, *16*, 89–112.

(36) Feng, H.; Vu, N. D.; Zhou, Z.; Bai, Y. *Biochemistry* **2004**, *43*, 14325–14331.

net value of $\Delta V_{\ddagger-F}$ (-22 mL/mol). A significant enhancement of hydration of the TSE accounts for its similar κ_{\ddagger} value relative to F (Figure 3c); thus, the increased compressibility of the TSE (relative to F) that results from its less compact structure is offset by increased hydration and by retention of only a very small compressible water inaccessible core. Interestingly, such an interpretation is in good agreement with the temperature-dependent study of the protein,²¹ where it was found that the folding barrier is entropic ($\Delta H_{\ddagger-U} = -3$ kcal/mol vs $-T\Delta S_{\ddagger-U} = +7$ kcal/mol). The large entropic barrier was interpreted in terms of a decrease in chain entropy associated with folding to a reasonably compact TSE, without a significant release of water that would compensate the entropy loss. Taken together, the pressure- and temperature-dependent relaxation dispersion data suggest that the predominant release of water likely occurs after the formation of the rate-limiting step of folding for F61A/A90G Rd-apocyt b_{562} , as has been postulated for SH3 domain folding.³⁷

In summary, we have presented a volumetric analysis of the folding reaction of F61A/A90G Rd-apocyt b_{562} using relaxation dispersion NMR spectroscopy in conjunction with densimetric and ultrasonic velocity measurements. In the NMR approach, the folding/unfolding equilibrium is monitored as a function of pressure, without the need for the addition of denaturants. Folding and unfolding rates can be measured at each pressure, under equilibrium conditions. Because of the exquisite sensitivity of the dispersion profiles to pressure, only low-pressure values are required to observe measurable changes in rates, thereby avoiding potential complications that result from high-pressure-

induced changes to the U state ensemble and minimizing any changes to the folding mechanism that pressure might introduce. Although marginally stable proteins must be employed using this approach (with populations of the U state greater than approximately 0.5%), in our experience, it is easy to produce such molecules and there are many such systems available for analysis. Notably, reasonable agreement between $\Delta\kappa_{S,U-F}$ and $\Delta\kappa_{T,U-F}$ values has been obtained (with $\Delta\kappa_{S,U-F}$, $\Delta\kappa_{T,U-F} < 0$), unlike many other studies where high pressures are employed. The measured volume and compressibility changes of the TSE relative to the U state provide a picture of the TSE that is significantly more detailed than that obtained exclusively from more conventional temperature-dependent folding studies.

Acknowledgment. D.M.K. and I.B. acknowledge support in the form of Canadian Institutes of Health Research (CIHR) postdoctoral and predoctoral (Training Program in Protein Folding) fellowships. This work was supported by the Natural Sciences and Engineering Research Council of Canada (S.P., T.V.C., L.E.K.), the CIHR (T.V.C and L.E.K.), the Petroleum Research Fund of the ACS (T.V.C.), and the intramural program of the National Institutes of Health, CCR, NCI (Z.Z. and Y.B.). L.E.K. holds a Canada Research Chair in Biochemistry.

Supporting Information Available: Pressure dependence of relaxation dispersion profiles for several residues of F61A/A90G Rd-apocyt b_{562} (600 MHz spectrometer field, 45 °C). This material is available free of charge via the Internet at <http://pubs.acs.org>.

(37) Shea, J. E.; Onuchic, J. N.; Brooks, C. L., III. *Proc. Natl. Acad. Sci. U.S.A.* **2002**, *99*, 16064–16068.

JA0601540